6th European Conference on Computational Mechanics (ECCM 6)
7th European Conference on Computational Fluid Dynamics (ECFD 7)
1115 June 2018, Glasgow, UK

ENTROPY PRODUCTION IN NEAR-WALL TURBULENT FLOW INSIDE A GENERIC AIR-TO-AIR PLATE HEAT EXCHANGER

F. RIES[1], Y. LI[1] AND A. SADIKI[1,2]

[1] Institute of Energy and Power Plant Technology
Technische Universität Darmstadt, 64287 Darmstadt, Germany
yongxiang.li@ ekt.tu-darmstadt.de, www.ekt.tu-darmstadt.de

[2] Laboratoire de Genies des Procedes et Thermodynamique,
Institut Superieur des Sciences et Techniques Appliquees,
Ndolo Kinshasa, RD Congo

Key words: heat recovery, energy efficiency, irreversibility, entropy production, direct numerical simualtion

Abstract. In this paper, the degree of thermodynamic ineffectiveness of an air-to-air heat recovery system has been investigated based on second law analysis. For this purpose, direct numerical simulation (DNS) of a generic air-to-air plate heat exchanger at a moderate Reynolds number of $Re = 5500$ has been carried out. At first, thermal and fluid flow properties are examined and compared with reference data from the literature. Then, entropy production rates evolving during the thermofluid processes are investigated in order to identify the causes of irreversibilities in such thermal devices. Thereby, it turned out that vigorous turbulent activity of heat and fluid flow appears in the vicinity of the heated wall associated with high turbulent production and dissipation rates while at the same time the heated wall acts as a strong source of irreversibility with high entropy generation for both, entropy production by viscous dissipation and by heat transfer across a finite temperature difference. This suggests that the thermodynamic ineffectiveness of such devices is caused primarily by the near-wall region and not by thermofluid processes evolving in the outer region. Finally, a dataset of local rates of entropy production by viscous dissipation and heat transfer is provided that is very difficult to obtain experimentally and might be of particular interest for the validation of large eddy and Reynolds-averaged Navier-Stokes modeling approaches that are frequently used for the conceptual design of air-to-air plate type heat exchangers.

1 INTRODUCTION

Heating, ventilation and air conditioning account for approximately $40\% - 60\%$ of the total energy consumption in buildings [1] and is responsible for more than 15% of the worldwide carbon emission [2]. It is therefore not surprising that a wide range of processes

and equipments have been developed to minimize energy consumption of buildings. One of them is waste heat recovery which is frequently applied to reduce the heating and cooling demands of buildings. Thereby, thermal energy from exhaust air is transfered to incoming fresh air (or vice versa in the case of cooling) by means of air-to-air heat exchangers. Depending on the technical requirements, different types of heat exchangers are utilized for waste heat recovery like rotary wheel heat exchangers, heat pipes, run around heat exchangers or plate type heat exchangers. Reviews of recent development of air-to-air heat recovery technologies can be found in [2, 3, 4, 5] and others.

Because of their high efficiency, most common type of heat recovery devices being used in practice are plate type heat exchangers. In this kind of heat exchangers, exhaust air and fresh air streams are divided by thin plates stacking together with small spacing between the plates to form thin flow channels [5]. Thermal energy is transfered via the plate heat exchanger surfaces from one air stream to the other. Thereby, the plates maybe smooth or may have some form of corrugation [5] and the airflow arrangement can be counter flow, cross flow or parallel flow [2]. Unfortunately, it has come to recognized that the effectiveness of sensible heat transfer depends on a large number of parameters in such devices like plate types, distance between the plates, pitch and orientation of corrugation and chevron angles, flow pattern, Reynolds number, fluid properties, and many more, that impede the conceptual design of efficient and compact air-to-air plate heat exchangers. For this purpose, several experiments have been carried out in the past to examine the influence of different design parameters of the performance of plate heat exchangers [6, 7, 8]. Furthermore, many researchers used Reynolds-averaged Navier-Stokes (RANS) [9, 10, 11, 12] and scale resolved simulations [13, 15, 16] technique in order to complement these experimental results.

Although air-to-air heat exchangers have been the subject of extensive research in the last decades and are widely employed for waste heat recovery in buildings, very little is known about irreversibilities evolving in such thermal devices. Thermodynamic irreversibilities in thermofluid processes, which can be expressed by means of entropy production rates, manifests itself through local degradation or loss of degrees of freedom in the system behavior or in the turbulence structure of a flow, and manifests itself as a monotonous increase in disorder in the system [17, 18, 19]. From an engineering standpoint, the concept of entropy generation minimization can be useful or even necessary as a design tool in order to avoid the imminent loss of available mechanical power [20, 21], likewise in the design of air-to-air plate type heat exchanger. Therefore, for efficient use of energy, the designer must know the irreversibility picture of the thermal device in order to reduce its degree of thermodynamic ineffectiveness. This concept of thermodynamic irreversibility and its relation to the one-way destruction of available work are not new [20], however entropy generation maps for application with practical relevance are most often not available in the literature. This motivates the present study which intends to provide an entropy generation map of an generic air-to-air plate type heat exchangers based on direct numerical simulation technique.

This paper is organized as follows. In section 2, the numerical methods and the second law of thermodynamics in the form of entropy transport equation are introduced. Next,

the configuration investigated in this work, a generic air-to-air plate type heat exchanger is described in section 3. The achieved results are presented and discussed in section 4. Finally, some concluding remarks are given in section 5.

2 METHODS

DNS of incompressible turbulent channel flow with convective heat transport and constant physical properties has been carried out. Thereby, temperature is treated as a passive scalar and buoyancy effects are neglected. By means of this assumptions, the governing equations applied are the continuity equation

$$\frac{\partial U_i}{\partial x_i} = 0, \tag{1}$$

the momentum equation

$$\frac{\partial U_i}{\partial t} + \frac{\partial}{\partial x_j}\left(U_i\, U_j\right) = -\frac{\partial p}{\partial x_i} + \frac{\partial}{\partial x_j}\left(\nu\left(\frac{\partial U_i}{\partial x_j} + \frac{\partial U_j}{\partial x_i}\right)\right), \tag{2}$$

and the energy equation in form of temperature transport equation

$$\frac{\partial T}{\partial t} + \frac{\partial}{\partial x_j}\left(U_j\, T\right) = \frac{\partial}{\partial x_i}\left(\frac{\nu}{Pr}\frac{\partial T}{\partial x_i}\right). \tag{3}$$

Here, U_i are the local velocity components, p is the local hydrodynamic pressure, T the local temperature, ν the kinematic viscosity and Pr the molecular Prandtl number, which is set to $Pr = 0.71$ in the present study corresponding to the value of air at standard conditions.

In order to display irreversibilities within a turbulent flow with convective heat transport, the second law of thermodynamics in form of local entropy imbalance at the continuum level is used following [20, 22, 17, 23]. In the case of single phase, non-reacting, single component fluid flow with Fourier heat conduction and no external body force, the local entropy imbalance reads [21]

$$\frac{\partial \rho s}{\partial t} + \frac{\partial \rho U_j s}{\partial x_j} + \frac{\partial}{\partial x_j}\left(\frac{q_j}{T}\right) = \underbrace{\frac{\rho\nu}{T}\left(\frac{\partial U_i}{\partial x_j} + \frac{\partial U_j}{\partial x_i}\right)\frac{\partial U_i}{\partial x_j}}_{\Pi_v} + \underbrace{\frac{\lambda}{T^2}\frac{\partial T}{\partial x_j}\frac{\partial T}{\partial x_j}}_{\Pi_q} \geq 0, \tag{4}$$

where s is the entropy density, λ the thermal conductivity, Π_v the local rate of entropy production by viscous dissipation and Π_q the local entropy production rate by heat transport. Here, it is assumed that inequality 2 holds at any position in space and time and Π_v and Π_q are always non-negative, such that the entropy imbalance holds. Note that equation 4 goes beyond the usual formulation of the second law in equilibrium thermodynamics where only the global increase of entropy between two equilibrium states in an isolated system is considered [24].

The governing equations 1-3 are solved numerically using a low-dissipative projection method [25] with a three-stages explicit Runge-Kutta time integration scheme of second

order accuracy [26], which were added to the open source C++ library OpenFOAM 2.4.0. Regarding entropy production rates, Π_v and Π_q are calculated for each time step and averaged over time. A second order central differencing scheme is used for the convection term of the momentum equation and a second order, conservative scheme is utilized for the Laplacian and gradient terms. Concerning passive scalar fluxes, a second order minmod differencing scheme [27] is applied to ensure total variation diminishing of the solution. A detailed code verification of the present numerical approach is provided in [28].

3 TEST CASE

Only the fresh air intake side of the generic air-to-air heat exchanger is considered in the present work. This consists of a full developed both side heated channel flow at $Re_\tau = 180$ based on the friction velocity and $Re_b = 5500$ based on the bulk velocity. A representation of the flow domain is sketched in figure 1.

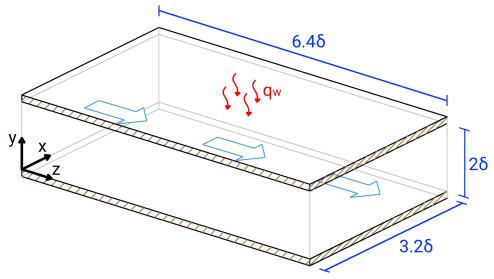

FIGURE 1. Computational domain and dimensions.

TABLE 1. Computational conditions.

Re_τ	180
Re_b	5500
Pr	0.71
domain size	$3.2\delta \times 2\delta \times 6.4\delta$
grid points	$161 \times 85 \times 161$
boundaries	periodic (x,z-direction), no-slip (y-direction), $T_w = 500K$

The computational domain applied in this work has a height $\delta = 0.01m$, a width of 3.2δ and a length of 6.4δ. A three-dimensional block-structured grid with $161 \times 85 \times 161$ grid points is used, which is refined towards the wall to ensure a non-dimensional wall distance smaller than one.

An isotropic turbulent velocity field is used to initialize the channel simulation. Therefore, a random velocity field is generated in physical space with a mean value of zero. In order to fulfill the continuity equation in Fourier space, the random field is cross-multiplied with the wavenumber vector and rescaled. In the next step, an autocorrelation spectrum similar to that found in [29] is imposed on each velocity component and the resulting random field is multiplied with a random phase. Finally, an inverse Fourier transformation is carried out leading to the initial fluctuation field. To avoid any uncertainties caused by the initial transient, five flows through the domain were solved before averaging was started.

Periodic boundary conditions are applied at the x- and z-direction. At the walls no-slip conditions are set for the velocity and a Dirichlet condition is imposed in the case of temperature. The pressure and temperature gradient that drives the heat and fluid flow is adjusted dynamically to maintain a constant mass flux and mean mixed temperature, respectively. Therefore, the pressure and temperature is split into a periodic and a non-

periodic part. A source term for the non-periodic part is added to the momentum and temperature equation, respectively (see [30]).

4 RESULTS

In the following, thermal and fluid flow properties are analyzed in order to characterize the general heat and flow pattern of the generic air-to-air plate type heat exchanger. Then, local entropy production rates are presented and correlated with the related flow and thermal results.

4.1 Thermal and Fluid Flow Properties

Figure 2 shows mean and rms values of the velocity and non-dimensional temperature as a function of non-dimensional wall distance y^+. Thereby, the non-dimensional temperature is defined as $\theta^+ = (T_w - T)/T_\tau$, where $T_\tau = q_w/(\rho c_p u_\tau)$ is the friction temperature and q_w the heat flux from both walls ($q_w = 1180K/m$). For comparison reference DNS data from the literature [30] are used.

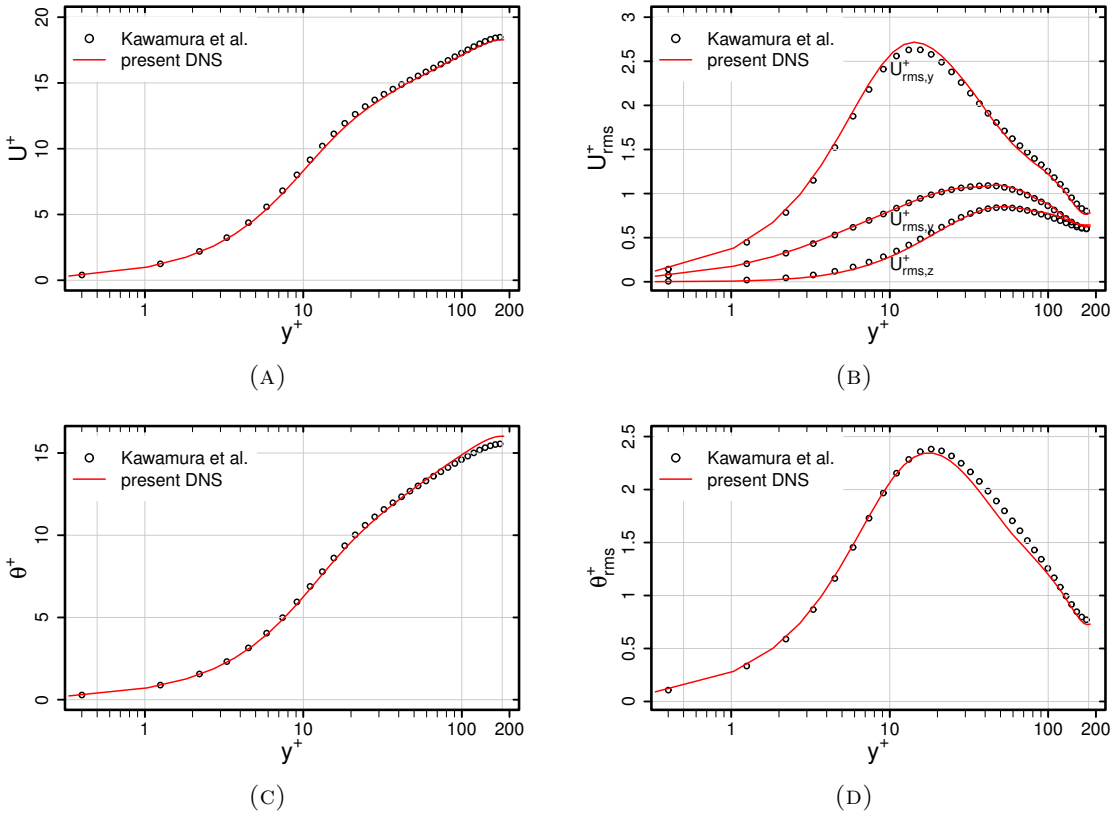

FIGURE 2. Mean (A), (C) and rms (B), (D) velocities and temperature as function of the non-dimensional wall distance y^+. Comparison of results from the present DNS with the reference data of [30].

As expected, mean values of the velocity (A) and dimensionless temperature (C) are small in the vicinity of the wall and increase rapidly apart from it. Both profiles exhibit a characteristic viscous sublayer region ($y^+ < 5$), a buffer layer region ($3 < y^+ < 30$), and a log-law region ($y^+ > 30$). Regarding velocities (B) and temperature (D) fluctuations, highest values appears within the buffer layer region (peak values at $y^+ \approx 20$), while they are negligible small in the viscous sublayer ($y^+ < 5$). Furthermore, mean and rms profiles agree very well with the reference DNS dataset of [30]. This establishes the validity of the present DNS results and confirms that the numerical method applied is appropriate to describe the thermofluid processes inside the generic air-to-air heat exchanger configuration.

Next, the evolution of the turbulent kinetic energy and temperature variance are analyzed in figure 3 (A) and (B), respectively, in order to identify and quantify the turbulence and heat transport phenomena that are not directly described by mean and rms values. Thereby, budget terms of the turbulent kinetic energy are normalized by ν/u_τ^4 and budget terms of temperature variance by $\nu/(u_\tau^2 T_\tau^2)$, where u_τ is the friction velocity.

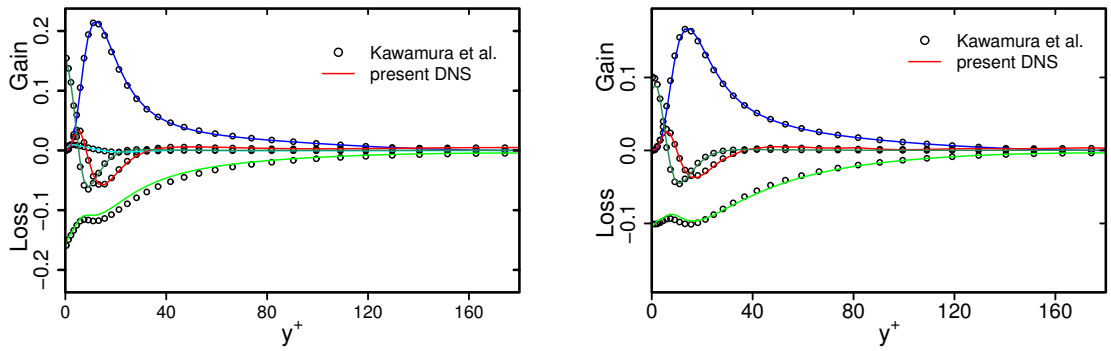

FIGURE 3. Normalized budget terms of turbulent kinetic energy (A) and temperature variance (B) as a function of dimensionless wall distance y^+. Comparison of results from the present DNS with the reference data of [30]. (—): production; (—): dissipation; (—): turbulent diffusion; (—): molecular diffusion; (—): pressure-related diffusion.

It can be seen in figure 4, that the balance of budget terms of turbulent kinetic energy and temperature variance are very similar. Throughout the heated channel, production and dissipation are the dominant terms, while pressure related diffusion is negligible small. Furthermore, all contribution terms are small far away from the wall and increase rapidly within the thermo-viscous boundary layer. Production reaches it peak value at $y^+ \approx 20$ and is predominantly balanced by dissipation. At the wall, production vanish, while dissipation is high and being balanced by molecular diffusion only. Obviously, turbulent thermofluid processes within air-to-air plate heat exchangers are dominated by near-wall effects rather than free-stream turbulence.

Finally, imprints of the instantaneous skin-friction coefficient $C_f = 2\tau_w/(\rho U_b^2)$ and

Nusselt number $Nu = \frac{\frac{\partial T}{\partial y}\delta}{2(T_w - T_\infty)}$ at the plate heat exchanger surface are depicted in figure 4 (A) and (B), respectively.

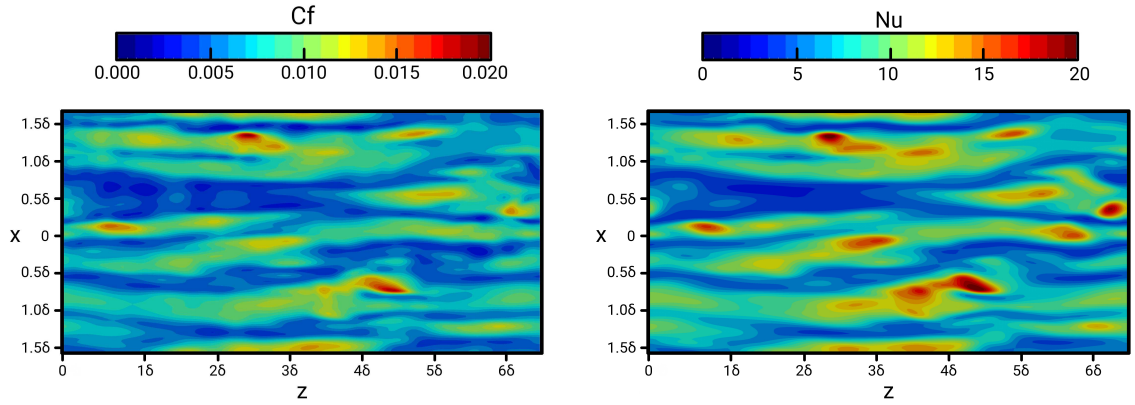

(A) (B)

FIGURE 4. Imprints of instantaneous skin-friction coefficient (A) and Nusselt number (B) at the plate heat exchanger surface.

By comparing figures 4 (A) and (B), it is interesting to observe that the imprints of instantaneous skin-friction coefficient and Nusselt number have a very similar organization. Thereby, large coherent streaks of concentrated C_f and Nu appear that are orientated in flow direction and extremely elongated. Furthermore, fluctuations are high which indicates strong transient heat and fluid flow processes in the vicinity of the wall, which again suggest that turbulent thermofluid processes within air-to-air plate heat exchangers are dominated by near-wall effects.

4.2 Entropy Production Mechanisms

After examining general thermal and fluid flow properties inside the generic air-to-air plate type heat exchanger, entropy generation mechanisms are analyzed now in order to identify and quantify the causes of irreversibilities in such thermal devices. Beginning with the visual appearance, figure 5 depicts instantaneous entropy production rates by viscous dissipation (A) and heat transport (B). Thereby, entropy production by viscous dissipation Π_v is normalized by $T_\tau \nu/(\rho u_\tau^4)$ and Π_q by $2\nu T_\tau^2 \lambda/(\rho c_p Pr)$. Notice that a logarithmic color scale is used in order visualize the wide range of entropy scales evolving in this configuration.

In terms of dimensionless rates of entropy production, it appears that entropy is primarily produced by viscous dissipation rather than heat transport. Thereby, large coherent streaks with high values of Π_v^+ and Π_q^+ are generated at the wall. Theses structures are convected away from the wall and tend to smear out while they cascade into smaller ones. By comparing Π_v^+ and Π_q^+, it is apparent that scales of Π_q^+ are considerable larger than scales of Π_v^+. This makes clear that irreversibilities in air-to-air plate type heat exchanger

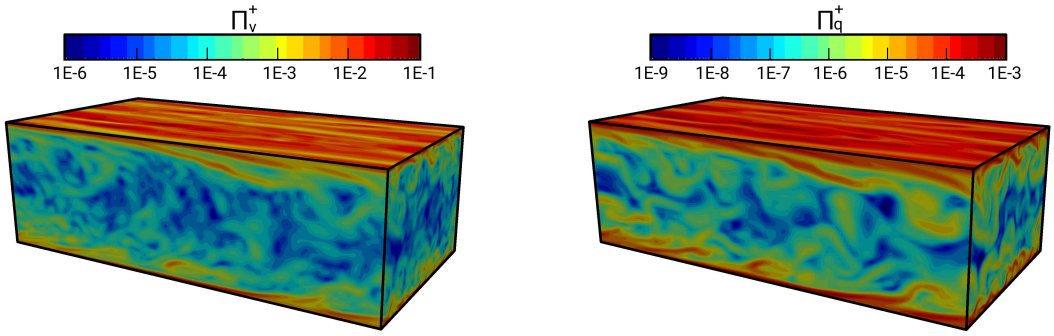

(A) (B)

FIGURE 5. Instances of entropy production rates by viscous dissipation (A) and heat transfer (B) inside the generic heat exchanger.

occur on different scales, but primarily on large scales in the case of heat transport and over a wide range of scales in the case of viscous dissipation.

Next, the observations from the visual appearance are quantified by means time-averaged rates of entropy production as a function of non-dimensional wall distance y^+ in figure 6.

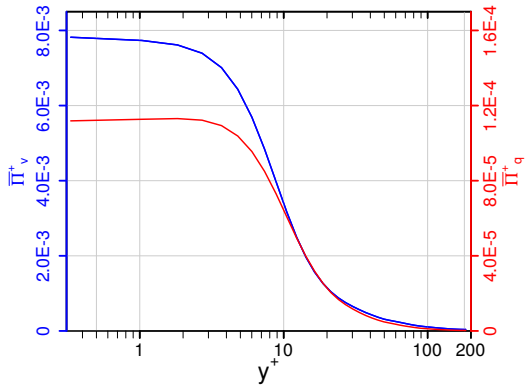

FIGURE 6. Instances of entropy production rates by viscous dissipation (A) and heat transfer (B) inside the generic heat exchanger.

Both, Π_v^+ and Π_q^+ are high at the viscous sublayer ($y^+ < 5$), decrease rapidly within the buffer layer ($y^+ < 30$) and are low at the log-law region ($y^+ > 30$). This is in good agreement with the observations in subsection 4.1 that turbulent thermofluid processes within air-to-air plate heat exchangers are predominantly limited to the near-wall region and as it can be seen here, these processes are essentially irreversible. Based on this, it can be concluded that the degree of thermodynamic ineffectiveness of air-to-air plate type heat exchangers are highly influenced by the near-wall region which acts as a strong source of irreversibility. Therefore, for efficient use of energy in such thermal devices, the design of the plate types are of crucial importance.

5 CONCLUSIONS

Direct numerical simulation of a generic air-to-air plate type heat exchanger has been carried out in order to investigate the degree of thermodynamic ineffectiveness of such thermal devices frequently used for waste heat recovery in buildings. Thereby, several distinctive features of heat and fluid flow along with the related entropy generation mechanisms have been pointed out. Some important observations from this numerical study can be outlined as follows:

- examining turbulent near-wall flow statistics, it turned out that vigorous turbulent activity of heat and fluid flow appears in the vicinity of the heated wall associated with high turbulent production and dissipation rates. Thereby, fluctuation of the skin-friction coefficient and Nusselt number are high which indicates additionally strong transient thermofluid processes.

- it appears that entropy is primarily produced by viscous dissipation rather than heat transport processes. Thereby irreversibilities occur on different scales, primarily on large scales in the case of heat transport and over a wide range of scales in the case of viscous dissipation.

- the degree of thermodynamic ineffectiveness of air-to-air plate type heat exchangers are highly influenced by the near-wall region which acts as a strong source of irreversibility. Therefore, for efficient use of energy in such thermal devices, the design of the plate types are of crucial importance.

REFERENCES

[1] Pérez-Lombard, L.; Ortiz, J.; Pout, C. A review on buildings energy consumption information. *Energy and Buildings* **2008**, *40*, 394–398. DOI. 10.1016/j.enbuild.2007.03.007

[2] Zeng, C.; Liu, S.; Shukla, A. A review on the air-to-air heat and mass exchanger technologies for building applications. *Renewable and Sustainable Energy Reviews* **2017**, *75*, 753–774. DOI. 10.1016/j.rser.2016.11.052

[3] O'Connor, D.; Calautit, J. K. S.; Hughes, B. R. A review of heat recovery technology for passive ventilation applications. *Renewable and Sustainable Energy Reviews* **2016**, *54*, 1481–1493. DOI. 10.1016/j.rser.2015.10.039

[4] Cuce, P. M.; Riffat, S. A comprehensive review of heat recovery systems for building applications. *Renewable and Sustainable Energy Reviews* **2015**, *47*, 665–682. DOI. 10.1016/j.rser.2015.03.087

[5] Mardiana-Idayu, A.; Riffat, S. B. Review on heat recovery technologies for building applications. *Renewable and Sustainable Energy Reviews* **2012**, *16*, 1241–1255. DOI. 10.1016/j.rser.2011.09.026

[6] Khan, T. S.; Khan, M. S.; Chyu, M.-C.; Ayub, Z. H. Experimental investigation of single phase convective heat transfer coefficient in a corrugated plate heat exchanger for multiple plate configurations. *Applied Thermal Engineering* **2010**, *30*, 1058–1065. DOI. 10.1016/j.applthermaleng.2010.01.021

[7] Gherasim, I.; Taws, M.; Galanis, N.; Nguyen, C. T. Heat Transfer and fluid flow in a plate heat exchanger part I. Experimental investigation. *International Journal of Thermal Sciences* **2011**, *50*, 1492–1498. DOI. 10.1016/j.ijthermalsci.2011.03.018

[8] Lu, Y.; Wang, Y.; Zhu, L.; Wang, Q. Enhanced performance of heat recovery ventilator by airflow-induced film vibration (HRV performance enhanced by FIV). *International Journal of Thermal Sciences* **2010**, *49*, 2037–2041. DOI. 10.1016/j.ijthermalsci.2010.06.001

[9] Han, X.-H.; Cui, L.-Q.; Chen, S.-J., Chen, G.-M.; Wang, Q. A numerical and experimental study of chevron, corrugated-plate heat exchangers. *International Communications in Heat and Mass Transfer* **2010**, *37*, 1008–1014. DOI. 10.1016/j.icheatmasstransfer.2010.06.026

[10] Kanaris, A. G.; Mouza, A. A.; Paras, S. V. Optimal design of a plate heat exchanger with undulated surfaces. *International Journal of Thermal Sciences* **2009**, *48*, 1184–1195. DOI. 10.1016/j.ijthermalsci.2008.11.001

[11] Ciofalo, M.; Stasiek, J.; Collins, M. W. Investigation of flow and heat transfer in corrugated passages -II. Numerical simulations. *International Journal of Heat and Mass Transfer* **1996**, *39*, 165–192. DOI. 10.1016/S0017-9310(96)85014-9

[12] Sarraf, K.; Launay, S.; Tadrist, L. Complex 3D-flow analysis and corrugation angle effect in plate heat exchangers. *International Journal of Thermal Sciences* **2015**, *94*, 126–138. DOI. 10.1016/j.ijthermalsci.2015.03.002

[13] Lee, J.; Lee, K.-W. Flow characteristics and thermal performance on chevron type plate heat exchangers. *International Journal of Heat and Mass Transfer* **2014**, *78*, 699–706. DOI. 10.1016/j.ijheatmasstransfer.2014.07.033

[14] Lee, J.; Lee, K.-W. Friction and Colburn factor correlations and shape optimization of chevron-type plate heat exchangers. *Applied Thermal Engineering* **2015**, *89*, 62–69. DOI. 10.1016/j.applthermaleng.2015.05.080

[15] Lee, J.; Lee, K.-W. Friction and Colburn factor correlations and shape optimization of chevron-type plate heat exchangers. *Applied Thermal Engineering* **2015**, *89*, 62–69. DOI. 10.1016/j.applthermaleng.2015.05.080

[16] Sohankar, A. Heat transfer augmentation in a rectangular channel with a vee-shaped vortex generator. *International Journal of Heat and Fluid Flow* **2007**, *28*, 306–317. DOI. 10.1016/j.ijheatfluidflow.2006.03.002

[17] Sadiki, A.; Hutter, K. On Thermodynamics of Turbulence: Development of First Order Closure Models and Critical Evaluation of Existing Models. *J. Non-Equilib. Thermodyn.* **2000**, *25*, 131–160, DOI. 10.1515/JNETDY.2000.009

[18] Ahmadi, G.; Cao, J.; Schneider, L.; Sadiki, A. A thermodynamical formulation for chemically active multiphase turbulent flows. *Int. J. Eng. Sci.* **2006**, *44*, 699–720, DOI. 10.1016/j.ijengsci.2006.06.001

[19] Turbulenzmodellierung und Thermodynamik, *Habilitationsschrift, TU-Darmstadt*, **1997**, *00*

[20] Bejan A. Second-law analysis in heat transfer and thermal design. *Adv. Heat Transf.* **1982**, *15*, 1–58.

[21] Bejan, A. *Entropy Generation Minimization: The Method of Thermodynamic Optimization of Finite-Size Systems and Finite-Time Processes*; CRC Press LLC: Boca Raton, FL, USA, 1995.

[22] Kock, F.; Herwig, H. Local entropy production in turbulent shear flows: A high-Reynolds number model with wall functions. *Int. J. Heat Mass Tran.* **2004**, *47*, 2205–2215.

[23] Ries, F.; Janicka, J.; Sadiki, A. Thermal Transport and Entropy Production Mechanisms in a Turbulent Round Jet at Supercritical Thermodynamic Conditions. *Entropy* **2017**, *19*, DOI. 10.3390/e19080404

[24] Jou, D.; Casas-Vázquez, J.; Lebon, G. *Extended Irreversible Thermodynamics*; Springer-Verlag Berlin Heidelberg New York: 2nd Edition,1993. ISBN 3-540-60789-7

[25] Chorin, A. J. Numerical Solution of the Navier-Stokes Equations. *Math Comput* **1968**, *22*, 745-762, DOI. 10.1090/S0025-5718-1968-0242392-2

[26] van der Houwen, P. J. Explicit Runge-Kutta formulas with increased stability boundaries. *Numer Math* **1972**, *20*, 149-164, DOI. 10.1007/BF01404404

[27] Roe, P. L. Characteristic-Based Schemes for the Euler Equations. *Annu Rev Fluid Mech* **1987**, *18*, 337-365, DOI. 10.1146/annurev.fl.18.010186.002005

[28] Ries, F.; Li, Y.; Rißmann, M.; Klingenberg, D.; Nishad, K.; Böhm, B.; Dreizler, A.; Janicka, J.; Sadiki, A. Database of near-wall turbulent flow properties of a jet impinging on a solid surface under different inclination angles. *Fluids* **2018**, *3(1)*, 5, DOI.10.3390/fluids3010005

[29] Erlebacher, G.; Hussaini, M. Y.; Speziale, C. G.; Zang, T. A. Toward the large-eddy simulation of compressible turbulent flows. *Journal of Fluid Mechanics* **1992**, *238*, 155–185, DOI. 10.1017/S0022112092001678

[30] Kawamura, H.; Abe, H.; Matsuo, Y. DNS of turbulent heat transfer in channel flow with respect to Reynolds and Prandtl number effects. *Int J Heat Fluid Fl* **1999**, *20*, 196-207, DOI. 10.1016/S0142-727X(99)00014-4